Available online at www.sciencedirect.com

SCIENCE DIRECT®

Journal of Catalysis 220 (2003) 468–477

JOURNAL OF CATALYSIS

www.elsevier.com/locate/jcat

Methane decomposition into hydrogen and carbon nanofibers over supported Pd–Ni catalysts

Sakae Takenaka,[a] Yukio Shigeta,[a] Eishi Tanabe,[b] and Kiyoshi Otsuka [a,*]

[a] *Department of Applied Chemistry, Graduate School of Science and Engineering, Tokyo Institute of Technology, Ookayama, Meguro-ku, Tokyo 152-8552, Japan*

[b] *Western Hiroshima Prefecture Industrial Institute, Kagamiyama, Higashi-Hiroshima, Hiroshima 739-0046, Japan*

Received 4 April 2003; revised 21 May 2003; accepted 21 May 2003

Abstract

The effect of the addition of different metals (Cu, Rh, Pd, Ir, and Pt) into supported Ni catalysts on the catalytic performance of methane decomposition into pure hydrogen and carbon was examined. The addition of Pd brought about considerable increases in the catalytic life and in the accumulated yields of hydrogen and carbon at the complete deactivation of the catalyst, while modification with the other metals decreased the yields compared to those for Ni/SiO_2. For the Ni catalysts modified with Pd, the appropriate preparation conditions of the catalysts, the effect of catalytic supports, and the optimum reaction temperature on the methane decomposition were examined. The hydrogen yield attained a high value, 16,000 mol_{H_2}/mol_{Pd+Ni}, when Pd and Ni were of a mole ratio $Pd/(Pd+Ni) = 0.5$ and a total loading $Pd + Ni = 37$ wt% on carbon nanofiber support. This yield is the highest among those reported so far. Methane decomposition over Ni catalysts modified with Pd produced carbon nanofibers with unique structures, i.e., branched carbon nanofibers. XRD studies on the Ni catalysts modified with Pd indicated the formation of Pd–Ni alloys. The alloys are responsible for the increase in the catalytic life and the formation of carbon nanofibers with unique structures.

Keywords: Supported Pd–Ni catalysts; Pure hydrogen; Carbon nanofibers; Pd–Ni alloys

---

1. Introduction

Hydrogen is expected to become an important energy carrier for sustained energy consumption with reduced impact on the environment. A hydrogen-based energy system is regarded as a viable and advantageous option for delivering high-quality energy services. Hydrogen should be used as a fuel for H_2–O_2 fuel cells because of the high efficiency of hydrogen energy to electricity as well as no emission of any pollutant gases. Traditionally, hydrogen is synthesized through steam reforming and/or partial oxidation of methane. The CO coproduced with hydrogen is converted to CO_2 through the shift reaction with H_2O in order to obtain relatively pure hydrogen. However, 1–3% of CO is inevitably contained in the hydrogen after the shift reaction of CO. If the hydrogen is utilized as a fuel for the polymer electrolyte fuel cells (PEFC), the concentration of CO should be decreased less than 20 ppm through the selective oxidation of CO. This purification of CO adds extra cost and system volume for the production of hydrogen for PEFC.

Methane decomposition into hydrogen and carbon is of current interest as an alternative route of hydrogen production [1,2]. Methane decomposition produces hydrogen only as a gaseous product. It is well known that supported Ni catalyst is one of the most effective among the catalysts tested so far [3–5]. We have already examined the catalytic performance of Ni catalysts supported on different supports and obtained the highest yields of hydrogen over $Ni(40\ wt\%)/SiO_2$ [6,7]. The catalyst decomposed methane actively at the early period of the reaction. However, the activity of the catalyst decreased gradually with time on stream and finally the catalyst was deactivated completely. Thus, the catalysts having a longer life should be explored. In addition, the supported Ni catalysts cannot decompose methane efficiently at temperatures higher than 923 K because of a very rapid deactivation after contact with methane, while they are very active for the reaction in the temperature range from 773 to 873 K [7]. The methane conversion in the methane

---

[*] Corresponding author.
E-mail address: kotsuka@o.cc.titech.ac.jp (K. Otsuka).

0021-9517/$ – see front matter
doi:10.1016/S0021-9517(03)00244-6

decomposition is restricted by thermodynamic equilibrium, for example, to 28, 51, 72, and 80% under atmospheric pressure at 773, 873, 973, and 1023 K, respectively, assuming that methane is converted into H_2 and graphite. Therefore, the catalysts which can decompose methane at temperatures higher than 923 K are required in order to obtain a high one-pass conversion of methane.

Methane decomposition over supported Ni catalysts produces carbon nanofibers accompanied by hydrogen production [8–10]. The synthesis of novel nanometer-scale materials is a major target in current material science research. One of the most fruitful and active fields in nanostructures is the preparation and characterization of carbon nanotube and carbon nanofibers, because of their attractive physical and chemical properties [11]. Carbon nanofibers are expected to be utilized, for example, as hydrogen storage materials, nanoelectrical devices, nanowires, and nanosensors [12].

In the methane decomposition over supported Ni catalysts, Ni metal particles on catalytic support decompose methane into carbon and hydrogen atoms [8]. Carbon atoms deposited on Ni metal surfaces would diffuse through the bulk of metal particles and/or on the metal surface to the precipitation sites to form graphitic layers, generating a carbon nanofiber. The Ni metal particles would be deactivated by coverage of the metal surfaces with graphite layers and the structural changes to some nickel carbide species [13]. This reaction mechanism implies that the catalytic life would be determined by the balance of the deposition rate of carbons from methane on the surface of Ni metal particles and the diffusion rate of carbon atoms through bulk or surface of metal particles. If Ni metal is modified with other metals, it is expected that the balance of deposition and diffusion rates of carbons would be changed, which may bring about the improvement in the catalytic performance of supported Ni catalysts. In addition, the modified Ni metal may grow carbon nanofibers with structures different from those formed on the unmodified one through methane decomposition [14,15].

In the present study, we have investigated the catalytic performance of supported Ni catalysts modified with other metal species for the methane decomposition. We report superior performance of supported Ni catalysts modified with Pd and the formation of carbon nanofibers with a unique structure.

2. Experimental

All the catalysts were prepared by a conventional impregnation method. MgO, Al_2O_3, SiO_2 (Cab-O-Sil, supplied from Cabot. Co.), TiO_2, and carbon nanofiber were utilized as catalytic supports in the present study. MgO (JRC-MGO1), Al_2O_3 (JRC-ALO4), and TiO_2 (JRC-TIO4) were supplied as reference catalysts from the Catalysis Society of Japan. The carbon nanofiber (denoted as CF hereafter) used in this study was homemade by the methane decomposition over Ni (5 wt%)/Cab-O-Sil at 823 K [13]. The specific surface areas of the CF, MgO, Al_2O_3, SiO_2, and TiO_2 were evaluated by the BET method (nitrogen adsorption at 77 K) to be 98, 52, 177, 200, and 40 m^2 g, respectively. $Ni(NO_3)_2$, $Cu(NO_3)_2$, $RhCl_3$, $PdCl_2$, $IrCl_3$, and H_2PtCl_6 were used as metal sources for the preparation of the supported metal catalysts. The catalytic support was impregnated with an aqueous solution containing these metal salts. The impregnated sample was dried at 373 K for 12 h.

Methane decomposition was carried out with a conventional gas-flow system. The catalyst (0.02–0.04 g) was spread on the flat bottom of a reactor (diameter = 3 cm and length = 20 cm) made from quartz. Prior to the reaction, the catalyst was reduced by hydrogen at 573 K for 1 h. After the reduction of the catalyst, hydrogen was flushed out with argon and methane was reacted with the catalyst at the required temperature. During the methane decomposition, a part of gases at the exit of the catalyst bed was sampled out and analyzed by GC.

X-ray diffraction (XRD) patterns were measured by a Rigaku RINT 2500V diffractometer using Cu-K_α radiation at room temperature.

SEM and TEM images of carbons deposited by the methane decomposition were measured using a Hitachi FE-SEM S-800 (field emission gun scanning electron microscope) and a JEOL JEM-3000F, respectively.

3. Results and discussion

3.1. Effect of different metals (M) added to Ni/SiO_2

Fig. 1 shows changes of methane conversions as a function of time on stream of methane in the methane decomposition over Ni/SiO_2, Pd/SiO_2, and the Ni/SiO_2 catalysts

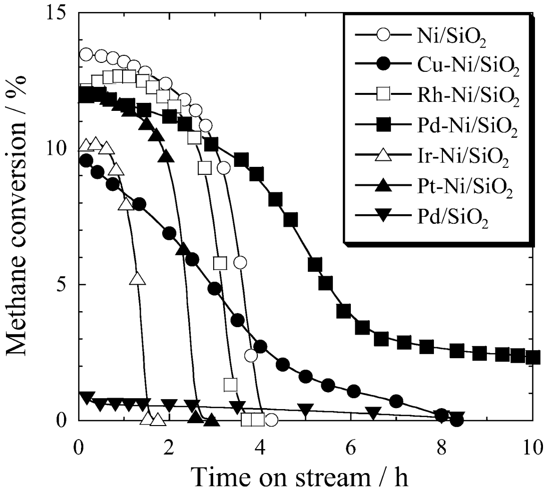

Fig. 1. Change of methane conversion as a function of time on stream of methane in the methane decomposition over Ni/SiO_2 modified with different metal species, Ni/SiO_2 and Pd/SiO_2. Reaction temperature = 823 K; catalysts = 0.040 g; CH_4 = 101 kPa and 40 ml/min.

modified with different metal species (M = Cu, Rh, Pd, Ir, and Pt). The reactions were performed at 823 K. The modified catalysts are denoted as M–Ni/SiO_2 hereafter. The loading of Ni in M–Ni/SiO_2 and Ni/SiO_2 was adjusted to 5 wt%. The molar ratio of the metal species (M) added to Ni/SiO_2 was 0.1 (M/Ni). For all the catalysts, methane decomposition proceeded selectively to form hydrogen only as a gaseous product. The addition of metal species into Ni/SiO_2 brought about slight decreases in the methane conversion at the initial period, irrespective of the kind of added metals. Methane conversion for Ni/SiO_2 was kept high until 2 h of time on stream. However, the conversion decreased quickly with the time on stream after 2 h and the catalyst was deactivated completely at ca. 4 h. The features of kinetic curves of methane conversion for Rh–, Ir–, and Pt–Ni/SiO_2 were similar to those for Ni/SiO_2. The catalytic activities of Rh–, Ir–, and Pt–Ni/SiO_2 declined gradually with time on stream and their activities were lost completely at 3.8, 3.0, and 1.8 h of time on stream, respectively. These results indicate that the addition of Rh, Ir, and Pt shortens the catalytic life of Ni/SiO_2 for the methane decomposition. In contrast, the addition of Cu and Pd improved the catalytic life of Ni/SiO_2. The catalytic activities of Cu– and Pd–Ni/SiO_2 declined gradually with time on stream in the same way as that of Ni/SiO_2. However, the decrease in methane conversion became moderate after 4 and 6 h for Cu–Ni/SiO_2 and Pd–Ni/SiO_2, respectively. Especially, the catalytic activity of Pd–Ni/SiO_2 decreased very gradually after 6 h and the complete deactivation was observed at ca. 50 h. The catalytic activity of Pd/SiO_2 was very low compared to those of Ni/SiO_2 and Pd–Ni/SiO_2. The loading of Pd in Pd/SiO_2 was adjusted to be the same as that in Pd–Ni/SiO_2. Therefore, the specific activity of the Pd–Ni/SiO_2 catalyst after 6 h of the time on stream cannot be explained by the sum of those of Ni/SiO_2 and Pd/SiO_2; i.e., the synergy of Ni and Pd is suggested.

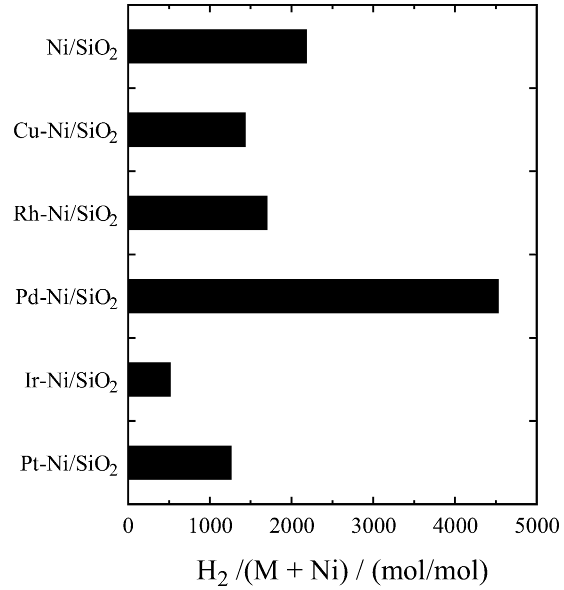

Fig. 2. Hydrogen yields in the methane decomposition over Ni/SiO_2 modified with different metal species and Ni/SiO_2.

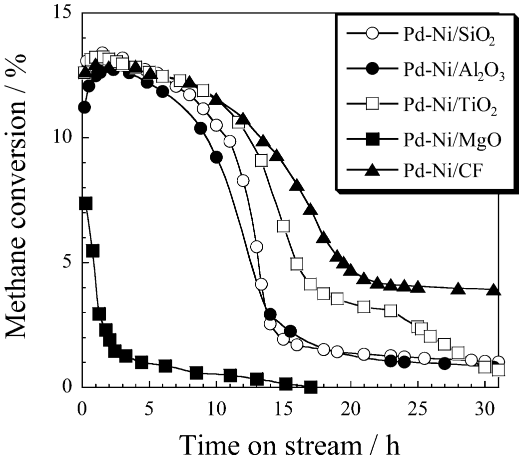

Fig. 3. Change of methane conversion as a function of time on stream of methane in the methane decomposition over Pd–Ni catalysts supported on different supports. Reaction temperature = 823 K; catalyst = 0.020 g; CH_4 = 101 kPa and 50 ml/min.

Fig. 2 shows hydrogen yields ($H_2/(M + Ni)$; moles of hydrogen formed per mole of the total metals (M + Ni) in the catalyst) at the complete deactivation of the catalyst. Carbon yield denoted as $C/(M + Ni)$ (moles of carbon deposited per mole of the total metals (M + Ni) in the catalyst) corresponds to a half of $H_2/(M + Ni)$. The yields were estimated from the kinetic curves of methane conversion shown in Fig. 1, assuming that methane decomposition to carbon and hydrogen proceeded stoichiometrically. Hydrogen yield for Ni/SiO_2 was evaluated to be 2184. The addition of metal species except for Pd resulted in decreases in the hydrogen yields. Avdeeva et al. reported the improvement of yields of hydrogen and carbon in the methane decomposition by addition of Cu into Ni/Al_2O_3 [16]. In the present study, the addition of Cu into Ni/SiO_2 brought about the elongation of catalytic life, but the yield for Cu–Ni/SiO_2 was lower than that for Ni/SiO_2. In contrast, the addition of Pd improved the hydrogen yield ($H_2/(Pd + Ni) = 4532$), which is more than twice that for Ni/SiO_2. These results shown in Figs. 1 and 2 indicate that the addition of Pd into Ni/SiO_2 improves the catalytic life and the yields of hydrogen and carbon in the methane decomposition. As will be described in detail later, we confirmed the formation of alloys between Pd and Ni for supported Pd–Ni catalysts. It is likely that Pd–Ni alloys bring about a long catalytic life and a high hydrogen yield in the methane decomposition. Hereafter, we paid our attention to Ni catalysts modified with Pd.

3.2. *Methane decomposition over Pd–Ni catalysts*

Fig. 3 shows changes of methane conversions as a function of time on stream of methane in the methane decomposition over Pd–Ni catalysts loaded on different supports. CF (carbon fiber), MgO, Al_2O_3, SiO_2, and TiO_2 were utilized as catalytic supports. For all the catalysts, the loadings of Pd and Ni were adjusted to be 2.5 and 27.5 wt%, respectively, which corresponds to a mole ratio of Pd/(Pd + Ni) = 0.05. The initial activity of Pd–Ni/MgO for the methane decomposition was peculiarly low compared to those of the other catalysts, while the initial activities of the other catalysts were almost the same level. We have already reported the methane decomposition over Ni (5 wt%) catalysts loaded on different supports [6]. The order of catalytic activity of Ni catalysts according to the kind of supports was similar to that of Pd–Ni catalysts, i.e., Ni/MgO showed a low activity for the methane decomposition, while the catalytic activities of Ni/TiO_2, Ni/SiO_2, and Ni/graphite were high. In the case of methane decomposition over supported Ni catalysts, we concluded that the difference in the catalytic activities among Ni catalysts on different supports could be explained by the state of Ni species. Most of Ni species in Ni/MgO were present as solid solutions, $NiMgO_x$, and they were not reduced easily into Ni metal, while Ni species in Ni/graphite, Ni/SiO_2, and Ni/TiO_2 were present as Ni metal mainly. It is generally accepted that Ni metal particles decompose methane and grow carbon nanofibers [8]. Thus, the catalytic activity of Ni/MgO for the methane decomposition was low. It is likely that the catalytic activity of Pd–Ni/MgO would also be low because Ni species in the catalyst form the $NiMgO_x$ solid solutions.

For all the supported Pd–Ni catalysts except for Pd–Ni/MgO in Fig. 3, similar kinetic curves of methane conversion were obtained. The methane conversions were higher than 10% until ca. 10 h of time on stream and then they declined significantly with time on stream. However, the decline was mitigated at 10–15 h and continuous conversions of methane were observed. These continuous conversions have not been observed so far in the methane decomposition over supported Ni catalysts [6,7,13]. Therefore, it is speculated that the alloys of Pd and Ni bring about this continuous reaction. The level of continuous methane conversion depended on the type of catalytic support, i.e., the conversion became higher in the order of Pd–Ni/CF > Pd–Ni/TiO_2 > Pd–Ni/SiO_2 > Pd–Ni/Al_2O_3.

The hydrogen yields for Pd–Ni catalysts supported on different supports were estimated from the kinetic curves of methane conversion from 0 to 30 h of time on stream shown in Fig. 3. The hydrogen yields were of the order as Pd–Ni/CF (5342) > Pd–Ni/TiO_2 (4764) > Pd–Ni/SiO_2 (4064) > Pd–Ni/Al_2O_3 (3558) ≫ Pd–Ni/MgO (572). Pd–Ni/CF kept the highest methane conversion (ca. 4%) at 30 h of time on stream among all the Pd–Ni catalysts, as can be seen in Fig. 3. Thus, if the reactions were continued for longer time, the hydrogen yield for the Pd–Ni/CF became far greater than those for the other catalysts. Thus, we have chosen Pd–Ni/CF for further studies on the effect of mole ratio of Pd and Ni, and of the loading of Pd and Ni on the methane decomposition.

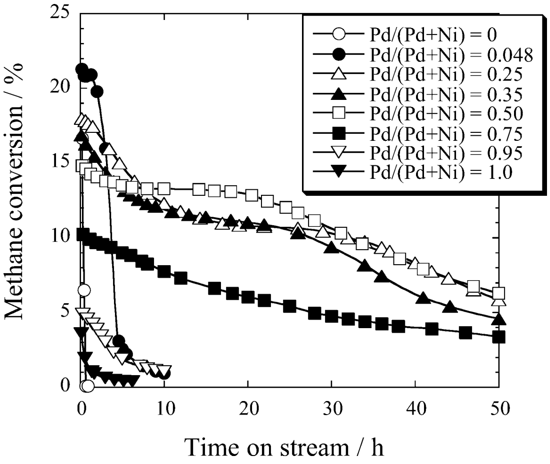

Fig. 4. Change of methane conversion as a function of time on stream of methane in the methane decomposition over Pd–Ni/CF catalysts with different mole ratios of Pd/(Pd + Ni). Reaction temperature = 873 K; catalyst = 0.020 g; CH_4 = 101 kPa and 50 ml/min.

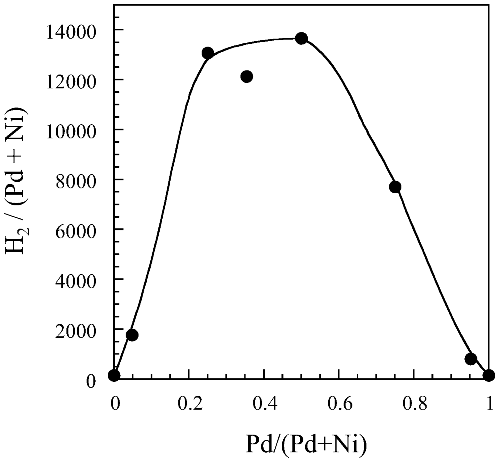

Fig. 5. Hydrogen yields in the methane decomposition over Pd–Ni/CF catalysts with different mole ratios of Pd/(Pd + Ni).

Fig. 4 shows changes of methane conversion with time on stream of methane over Pd–Ni/CF catalysts with different mole ratios of Pd/(Pd + Ni). The reactions were performed at 873 K. For all the fresh catalysts, the total mole of Pd and Ni loaded on the CF support was adjusted to be 7.8 mol% ((Pd + Ni)/(Pd + Ni + C) = 7.8 mol%). The hydrogen yields in the methane decomposition were estimated from the kinetic curves of methane conversion from 0 to 50 h of time on stream (Fig. 4). The hydrogen yields calculated are shown in Fig. 5. Ni/CF catalyst without Pd was deactivated immediately after the contact of methane at the reaction temperature (873 K), although the initial catalytic activity was high. Thus, the total hydrogen yield for Ni/CF became very low (H_2/Ni = 150) compared to the result at 823 K (Figs. 1 and 2). Pd/CF also showed a low activity and a low hydrogen yield (H_2/Pd = 150). On the other hand, Pd addition into Ni/CF changed the feature of kinetic curves of methane conversion. The initial conversion of methane decreased with higher mole ratios of Pd, which implies that the Pd–Ni alloys with a higher fraction of Pd show lower activity for the methane decomposition. It should be noted that the addition of Pd into Ni/CF extended the catalytic life for the

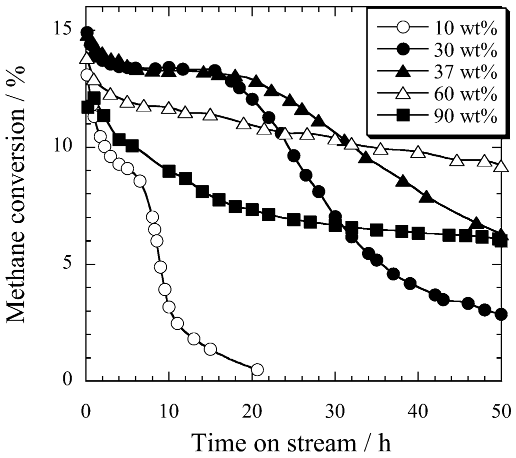

Fig. 6. Change of methane conversion as a function of time on stream of methane in the methane decomposition over Pd–Ni/CF catalysts with different loadings of Pd and Ni. Reaction temperature = 873 K; catalyst = 0.02 g; mole ratio of Pd/(Pd + Ni) = 0.5; CH_4 = 101 kPa and 50 ml/min.

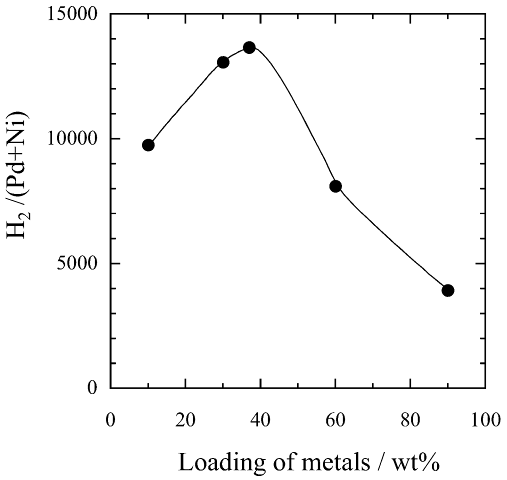

Fig. 7. Hydrogen yields in the methane decomposition over Pd–Ni/CF catalysts with different loadings of Pd and Ni.

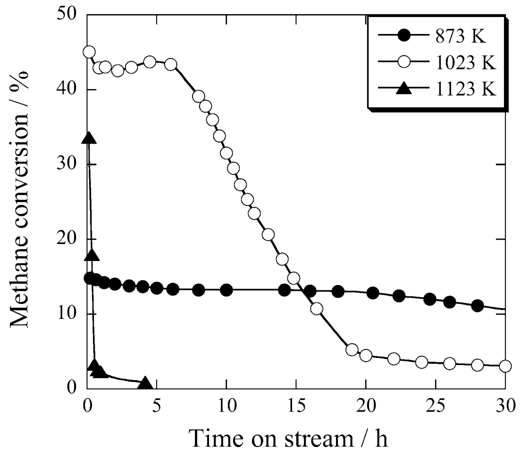

Fig. 8. Change of methane conversion as a function of time on stream of methane in the methane decomposition over Pd–Ni/CF catalysts at different temperatures. Catalyst, = 0.02 g; metal loading = 37 wt% (7.8 mol%); mole ratio of Pd/(Pd + Ni) = 0.5; CH_4 = 101 kPa and 50 ml/min.

methane decomposition remarkably irrespective of the mole ratio Pd/(Pd + Ni). Especially, the Pd addition of the mole ratio Pd/(Pd + Ni) of 0.25 to 0.5 prolonged their catalytic lives dramatically. However, the addition of excess amounts of Pd (mole ratio Pd/(Pd + Ni) from 0.75 to 0.95) decreased the catalytic life. In addition, as can be seen in Fig. 5, the hydrogen yield increased significantly with an increase in Pd/(Pd + Ni) ratio from 0 to 0.2 and the yield attained the maximum at 0.5 of Pd/(Pd + Ni). The maximum hydrogen yield was ca. 14000 mol/mol of (Pd + Ni), which was about 90 times greater than those for Ni/CF and Pd/CF. It should be noted that the hydrogen yields in Fig. 5 were estimated from the kinetic curves of methane conversion from 0 to 50 h of time on stream. The catalysts with Pd/(Pd + Ni) of 0.25, 0.35, 0.50, and of 0.75 were still active at 50 h of time on stream in Fig. 4.

Fig. 6 shows changes of methane conversions with time on stream of methane over Pd–Ni/CF catalysts with different total loadings of Pd and Ni. For all the catalysts, the Pd/(Pd + Ni) molar ratio was adjusted to 0.5 but the total amount of Pd and Ni was changed from 10 to 90 wt%. The catalysts with loadings of 37, 60, and 90 wt% were deactivated gradually with time on stream, while the catalyst of 10 wt% loading was deactivated quickly. In particular, the deactivation of the catalysts with loadings of 60 and 90 wt% was quite slow after 50 h of time on stream.

Fig. 7 shows the hydrogen yields estimated from the kinetic curves of methane conversion from 0 to 50 h of time on stream for Pd–Ni/CF with different total loadings of metals. We cannot discuss exactly the effect of loading of Pd and Ni on the hydrogen yield on the basis of the results shown in Fig. 7, because the catalysts with metal loadings higher than 30 wt% were still active at 50 h of time on stream. However, the most striking point is that even the catalyst with loading of 90 wt% showed a continuous and high conversion of methane or a high hydrogen yield. It is reasonable to consider that the particle size of metals should become larger with higher loadings of metal in the case of supported catalysts. We have already reported that in the methane decomposition over Ni/SiO_2, the catalytic activity and hydrogen yield were very low at a Ni loading of 90 wt%; i.e., the catalytic activity and life of Ni/SiO_2 for the methane decomposition are determined by the particle size of Ni metal [7]. However, Figs. 6 and 7 show a long life and a high yield of hydrogen even at a high loading of 90 wt% in the case of Pd–Ni/CF. It is likely that the catalytic methane decomposition over Pd–Ni alloys is not so sensitive to the particle size as the reaction over Ni metal without Pd.

Fig. 8 shows changes of methane conversions as a function of time on stream of methane for Pd–Ni/CF catalysts at different temperatures. The temperatures were changed from 873 to 1123 K. A Pd–Ni/CF sample with 37 wt% (7.8 mol%) of metal loading and 0.5 of Pd/(Pd + Ni) mole ratio was used for the reactions. The initial methane conver-

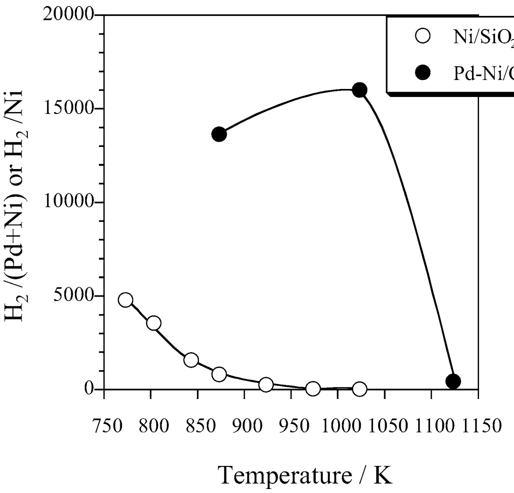

Fig. 9. Hydrogen yields in the methane decomposition over Pd–Ni/CF catalysts at different temperatures.

sions became higher when the temperature was raised from 873 to 1023 K. For the methane decomposition at 1023 K, the conversion was kept to ca. 43% for 7 h of time on stream but it decreased quickly with time on stream after 7 h. In contrast, the conversion at 873 K was kept almost constant (11–14%) for 30 h of time on stream. On the other hand, the catalyst was deactivated at 1123 K immediately after the reaction with methane. Fig. 9 shows the hydrogen yield in the methane decomposition over Pd–Ni/CF at different temperatures. The yields for the reactions at 873, 1023, and 1123 K were estimated from the kinetic curves of methane conversions in Fig. 8 from 0 to 50, 30, and to 4.2 h, respectively. The hydrogen yields for the methane decomposition over Ni (40 wt%)/SiO_2 (SiO_2; Kieselgel from Merck) at different temperatures are also shown in Fig. 9. The Ni (40 wt%)/SiO_2 (Kieselgel) was one of the most effective catalysts for the methane decomposition among all the supported Ni catalysts reported previously [7]. The hydrogen yields for the Ni (40 wt%)/SiO_2 (Kieselgel) were estimated after the complete deactivation of the catalyst for the methane decomposition, while the yields for Pd–Ni/CF at 873 and 1023 K were estimated before the complete deactivation of the catalyst. The Ni/SiO_2 showed a high hydrogen yield ($H_2/\mathrm{Ni} = 4806$) at 773 K; however, the yields decreased sharply with a rise in the reaction temperatures. In particular, the Ni/SiO_2 showed extremely low hydrogen yields ($H_2/\mathrm{Ni} < 60$) at temperatures higher than 973 K. In contrast, the hydrogen yields for the Pd–Ni/CF at 873 K and 1023 K were remarkably high. These results suggest that Pd–Ni/CF can catalyze the methane decomposition efficiently in a broad range of temperatures at < 1050 K, compared to Ni/SiO_2.

Fig. 10 shows the effect of contact time of methane with the Pd–Ni/CF catalyst on the methane decomposition. The specific formation rate of hydrogen and conversion of methane were plotted against W/F in the figure. The methane decomposition was performed at 1023 K over Pd–Ni/CF catalysts with 37 wt% (7.8 mol%) of metal loading and 0.5 of Pd/(Pd + Ni). In the reaction, weights of the catalyst (W) and flow rates of methane (F) were changed from 0.05 to 0.17 g and from 50 to 150 ml/min (STP), respectively, in order to adjust required W/F values. The specific formation rate of hydrogen per 1 g of the catalyst became higher as W/F values decreased. The specific rate attained 0.45 mol/(min g_{cat}) at $W/F = 0.035$ g_{cat}/l(STP) min, which corresponds to ca. 10 l(STP)/(min g_{cat}). The methane conversion increased with a rise in W/F. The conversion of methane increased to 70% at $W/F = 3.3$ g_{cat}/l(STP) min, which corresponds to a hydrogen concentration of 83 vol%. These results indicate that the Pd–Ni/CF is a quite active catalyst for the production of hydrogen by methane decomposition.

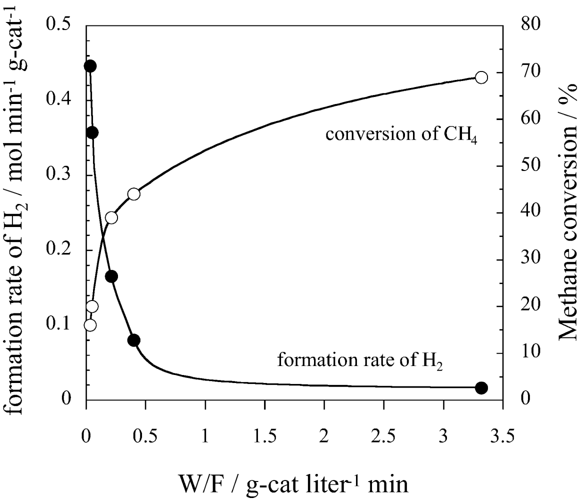

Fig. 10. Dependence of W/F on the formation rate of hydrogen and methane conversion in the methane decomposition over Pd–Ni/CF catalysts at 1023 K. Pd–Ni/CF: metal loading = 37 wt% (7.8 mol%); and mole ratio of Pd/(Pd + Ni) = 0.5.

As described earlier, supported Pd–Ni catalysts were effective for the methane decomposition at < 1050 K. The highest hydrogen yield obtained in this work was 16,000 mol/mol of (Pd + Ni) when the methane decomposition was performed at 1023 K for 30 h over Pd–Ni/CF catalysts with a Pd/(Pd + Ni) mole ratio of 0.5 and a total loading of Pd and Ni of 37 wt% (7.8 mol%), as shown in Figs. 8 and 9. The catalyst was still working at 30 h of time on stream as can be seen in Fig. 8. Thus, the total hydrogen yield until the complete deactivation of the catalyst will be greater than this value, if the reaction is performed for longer time. The maximum yields of hydrogen and carbon correspond to 390 g of hydrogen and 1170 g of carbon per 1 g of metals (Pd + Ni) in the catalyst. Recently, the Ni-based catalysts effective for the methane decomposition have been designed by several research groups. Avdeeva et al. reported yields of 92 g_{H_2}/g_{Ni} and 276 $g_{\mathrm{C}}/g_{\mathrm{Ni}}$ when the methane decomposition was performed over Ni (90 wt%)/Al_2O_3 modified with Cu of 3 at.% [16]. Ermakova et al. investigated the methane decomposition over the Ni/SiO_2 catalyst which was prepared by impregnation of NiO with an alcohol solution of tetraethoxysilane (TEOS) [17]. The highest yields, 128 g_{H_2}/g_{Ni} and 384 g_C/g_{Ni}, were obtained when SiO_2 was added by 10 wt% to Ni metal. We have recently reported yields of 164 g_{H_2}/g_{Ni} and 491 g_C/g_{Ni} in the methane decomposition over Ni (40 wt%)/SiO_2 (Kieselgel) [7]. Thus, the Pd–Ni/CF catalysts in Figs. 4 to 10 are quite effective for methane decomposition compared to others reported so far. In addition, the Pd–Ni/CF catalyst can catalyze the methane decomposition efficiently in a wide range of reaction temperatures at < 1050 K, while Ni/SiO_2 is deactivated immediately at temperatures higher than 873 K, as can be seen in Fig. 9. Therefore, the Pd–Ni/CF can be used at high temperatures in order to avoid the thermodynamic limitation for the production of concentrated hydrogen ($> 80\%$) by one-pass methane decomposition.

3.3. Characterization of Pd–Ni catalysts and carbons formed from methane

Fig. 11 shows XRD patterns of Ni/CF, Pd/CF, and Pd–Ni/CF. The loading of metal was adjusted to 7.8 mol% for all the catalysts. Prior to the measurement of XRD patterns, the catalysts were contacted with methane at 873 K for 10–20 min in order to examine the structure of metal species in these catalysts under the reaction conditions. For all the XRD patterns shown in Fig. 11, the diffraction lines due to CF support and carbons deposited from methane were found at $2\theta = 26$ and 43°, although the peak at 43° was very weak. For the XRD pattern of Ni/CF, the sharp diffraction lines due to Ni metal were observed at $2\theta = 44.5$ (Ni(111)) and 52.0° (Ni(200)), indicating that Ni species were present as Ni metal crystallites. As for the XRD pattern of Pd/CF, the sharp diffraction lines due to Pd metal were observed at $2\theta = 40.0$ (Pd(111)) and 46.5° (Pd(200)). Thus, the Pd species in Pd/CF were present as Pd metal crystallites. The addition of Pd into Ni/CF decreased or diminished the diffraction peaks due to Ni metal crystallites. It seems that the XRD pattern of Pd–Ni/CF of mole ratio 0.25 shows two wide diffraction patterns between the lines due to metallic Ni and Pd. For the XRD pattern of the catalyst of Pd/(Pd + Ni) = 0.5, two clear diffraction peaks appeared at $2\theta = 42.0$ and 49.0° and those due to metallic Ni and Pd disappeared. Each peak seems to be overlapped with broad diffraction spectra observed at $2\theta = 40$–44.5 and 46–52°, respectively. When the mole ratio Pd/(Pd + Ni) increased to 0.75, the diffraction lines at $2\theta = 42.0$ and 49.0° and those at 40.0 and 46.5° due to Pd metal were observed. The broad diffraction spectra at $2\theta = 40$–44.5 and 46–52° indicate the formation of Pd–Ni alloys. The results that the diffraction spectra due to Pd–Ni alloys were broad and those due to Ni and Pd metal were also observed in the XRD patterns of Pd–Ni/CF strongly suggest that the Pd/Ni ratio of the alloys must be widely distributed, i.e., the Pd–Ni alloys with different fractions of Pd and Ni could be present in addition to isolated Ni and Pd metals. In the case of bulk alloy formation, it is well known that Ni and Pd form homogeneous Pd–Ni alloys over the whole Pd/Ni composition range [18]. In the present study, the metal species in the Pd–Ni/CF were reduced with hydrogen at relatively low temperatures (573 K) in order to avoid the reduction of the support (CF) into methane. This reduction temperature of the catalyst might be too low to make uniform alloys of Pd and Ni. This is the reason why the XRD spectra for the Pd–Ni/CF catalysts in Fig. 11 gave broad diffraction lines at $2\theta = 40.0$–44.5 and 46.0 and 52°. However, it should be noted that the methane decomposition was performed at temperatures higher than 873 K. Therefore, we can expect that the Pd/Ni fraction in the metal particles on the support (CF) would become uniform during the reaction. In fact, the energy dispersive X-ray spectra (EDS) of the Pd–Ni catalyst after the methane decomposition at 873 K, which were measured at the same time as TEM images, showed that the Pd/Ni ratio in Pd–Ni alloys became uniform during the reaction. Therefore, we believe that the Pd–Ni alloys thus formed would show superior catalytic performance for methane decomposition, i.e., a longer life and high yields of hydrogen and carbon, as described earlier.

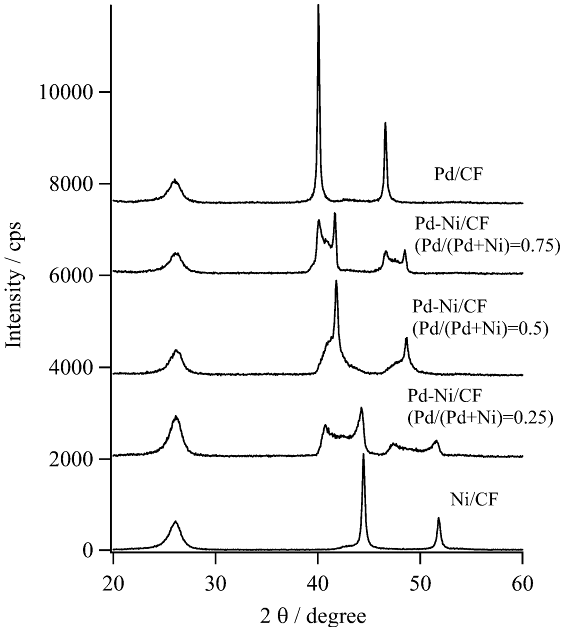

Fig. 11. XRD patterns of Ni/CF, Pd/CF, and Pd–Ni/CF with different mole ratios of Pd/(Pd + Ni). Metal loading = 7.8 mol%.

Fig. 12 shows SEM and TEM images of carbons deposited by the methane decomposition over Ni/CF and Pd/CF catalysts. The SEM and TEM images were measured after the reactions shown in Fig. 4. Because large amounts of carbons were deposited on both the catalysts by the methane decomposition, most of the carbons in the images were not of CF support but of the ones formed by the reaction. The SEM image for the Ni/CF (Fig. 12a) indicated the preferential formation of carbon nanofibers with relatively uniform diameters from 60 to 100 nm. From the TEM image for the Ni/CF (Fig. 12b), it was confirmed that a Ni metal particle was present at the tip of each carbon nanofiber, as many

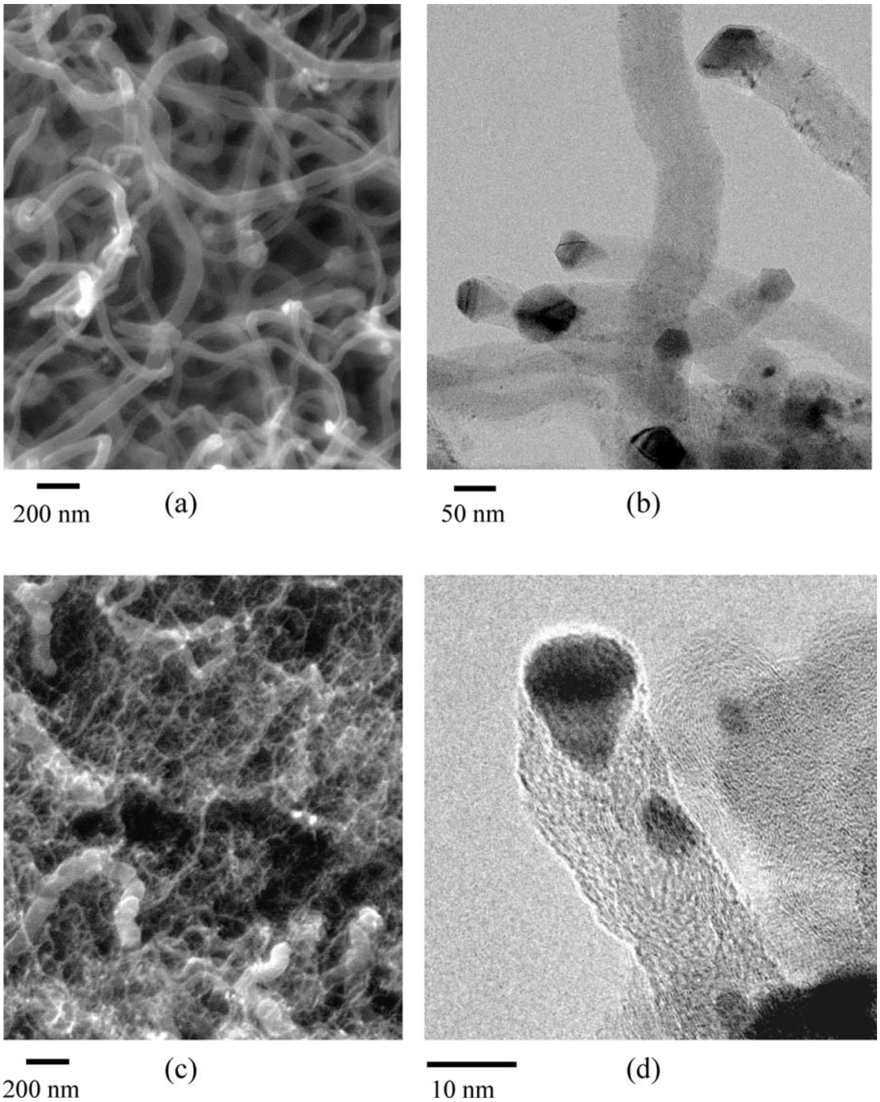

Fig. 12. SEM and TEM images of carbons deposited by the methane decomposition at 873 K over Ni/CF and Pd/CF. Loading of metal (Ni or Pd) = 7.8 mol%. SEM (a) and TEM images (b) for Ni/CF; SEM (c) and TEM images (d) for Pd/CF.

researchers already reported [8,13,19,20]. The Ni metal particles would decompose methane to grow carbon nanofibers. The Pd/CF catalyst also produced carbon nanofibers as can be seen in Fig. 12c, but their shapes were quite different from those on the Ni/CF. The diameter of carbon nanofibers on the Pd/CF ranged widely from 10 to 150 nm. A TEM image for the Pd/CF in Fig. 12d shows that a Pd metal particle was present at the tip of a carbon nanofiber. In addition, small Pd metal particles seem to be left in the fiber, while a Ni metal particle was always present at a fiber tip. However, we believed that the Pd metal particle at the tip of the carbon nanofiber is still responsible for fiber.

Fig. 13 shows SEM and TEM images of carbons deposited by methane decomposition over the Pd–Ni/CF catalyst of mole ratio $Pd/(Pd + Ni) = 0.5$. The SEM and TEM images were measured after the reactions shown in Fig. 4. Carbon nanofibers with a variety of diameters from 10 to 300 nm could be found in the SEM images for the Pd–Ni/CF (Fig. 13a). The most interesting observation is the formation of branched carbon nanofibers over the Pd–Ni/CF, as indicated in Fig. 13b. Carbon nanofibers similar to those on the Ni/CF and Pd/CF catalysts were also observed in Fig. 13a. The branched carbon nanofibers could not be found in the SEM and TEM images for the Ni/CF or Pd/CF. Thus, only the Pd–Ni alloys appear to produce branched carbon nanofibers. The formation of branched carbon nanofibers is a very rare case in the catalytic methane decomposition reported so far. The TEM images for the Pd–Ni/CF in Figs. 13c and d indicate the presence of Pd–Ni alloy particles. It was found that carbon nanofibers with and without branched structures grow from the alloy particles. The alloy particles seem to grow the carbon nanofibers in more than two directions, while particles of Ni and Pd metal grew those in one direction. It is suggested that several surfaces on a Pd–Ni alloy particle would grow carbon nanofibers, which might explain the formation of branched

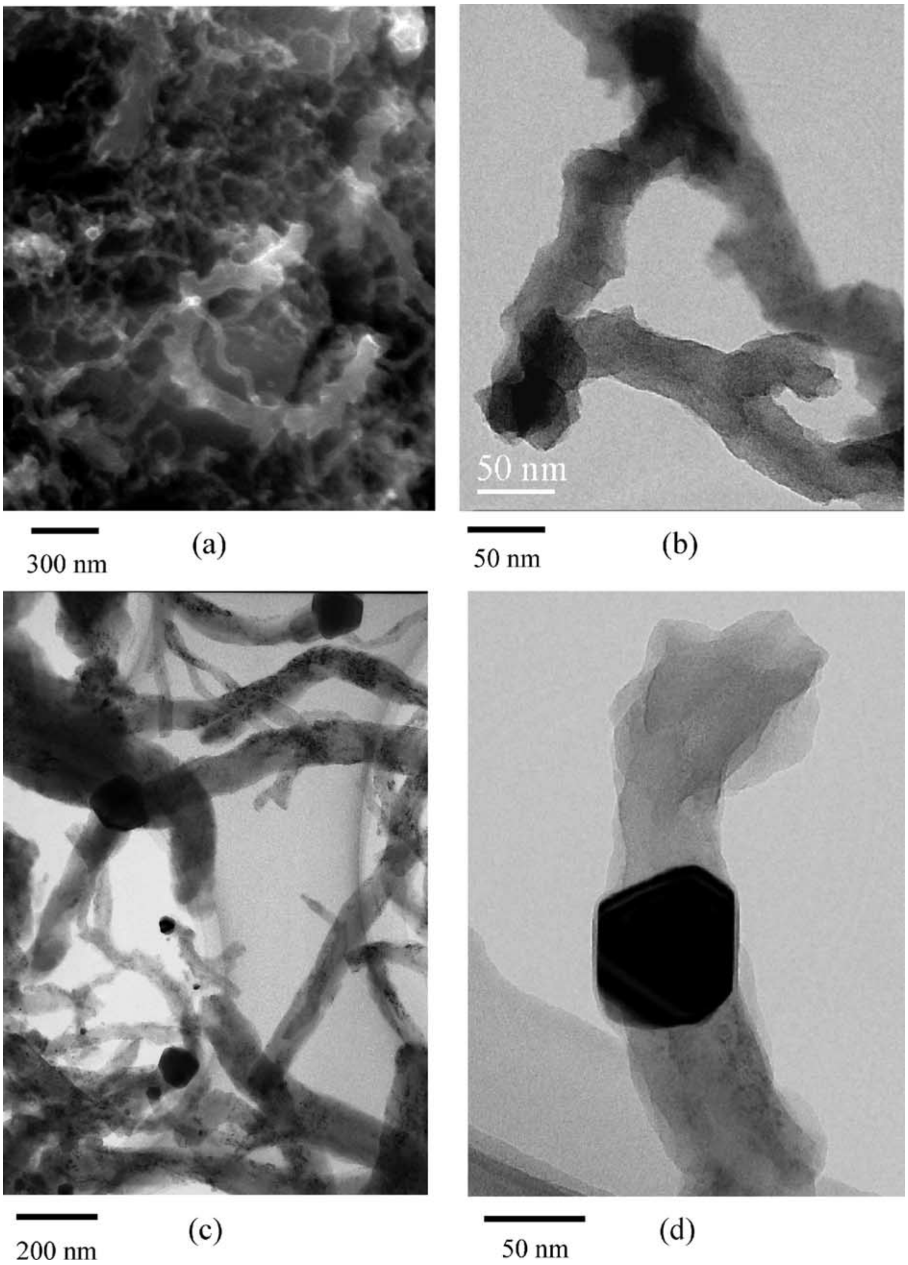

Fig. 13. SEM (a) and TEM images (b, c, d) of carbons deposited by methane decomposition at 873 K over Pd–Ni/CF. Loading of metal (Pd + Ni) = 7.8 mol%, mole ratio Pd/(Pd + Ni) = 0.5.

carbon nanofibers over the Pd–Ni/CF catalyst. These results suggest that the formation mechanism of carbon nanofibers for the Pd–Ni/CF is different from those for the Ni/CF and Pd/CF. We have already reported that Ni metal particles in supported Ni catalysts were transformed into nickel carbide species during the deactivation of the catalysts for methane decomposition [13]. This result implies that concentration of carbons in Ni metal particles becomes higher during the methane decomposition, which brings about the formation of stable nickel carbide species at the complete deactivation of the catalysts. In the case of Pd–Ni/CF catalysts, Pd–Ni alloys formed carbon nanofibers in several directions, while Ni metal particles formed fibers in one direction. It is likely that the concentration of carbon atoms in Pd–Ni alloys during methane decomposition is lower than that in Ni metal particles, because Pd–Ni alloys precipitate carbon atoms dissolved in the alloys from several surfaces of the alloys. Thus, life of Pd–Ni alloys for methane decomposition would be longer than that of Ni metal alone. However, we cannot discuss the formation mechanism further at the present stage. In the near future, we will report the chemical and physical properties of the carbon nanofibers formed by Pd–Ni catalysts and the formation mechanism of the fibers on the basis of the results by TEM, Raman spectroscopy, and X-ray absorption spectroscopy (XANES/EXAFS).

4. Conclusion

Based on the results described above, we conclude as follows:

1. Addition of Pd into supported Ni catalysts improved significantly the catalytic life and hydrogen yield for methane decomposition. The highest yields of hydrogen and carbon, 390 $g_{H_2}/g_{(Pd+Ni)}$ and 1170 $g_C/g_{(Pd+Ni)}$, were obtained by using the catalyst with mole ratio $Pd/(Pd+Ni)$ of 0.5 and total metal loading of 37 wt% on carbon nanofiber support.
2. Pd–Ni alloys were formed on supported Pd–Ni catalysts. The Pd–Ni alloys on various supports brought about a long life and a high hydrogen yield for the methane decomposition.
3. Methane decomposition over Pd–Ni/CF catalyst produced carbon nanofibers of unique structures, i.e., branched carbon nanofibers.

References

[1] Anonymous, Chem. Eng. 69 (1962) 90.
[2] N.Z. Muradov, Int. J. Hydrogen Energy 18 (1993) 211.
[3] T. Ishihara, Y. Miyashita, H. Iseda, Y. Takita, Chem. Lett. (1995) 93.
[4] T.V. Choudhary, C. Sivadinarayana, C.C. Chusuei, A. Klinghoffer, D.W. Goodman, J. Catal. 199 (2001) 9.
[5] K. Otsuka, S. Kobayashi, S. Takenaka, Appl. Catal. A 190 (2000) 261.
[6] S. Takenaka, H. Ogihara, I. Yamanaka, K. Otsuka, Appl. Catal. A 217 (2001) 101.
[7] S. Takenaka, S. Kobayashi, H. Ogihara, K. Otsuka, J. Catal. 217 (2003) 79.
[8] R.T.K. Baker, Carbon 27 (1989) 315.
[9] K. Otsuka, T. Seino, S. Kobayashi, S. Takenaka, Chem. Lett. (1999) 1179.
[10] R. Aiello, J.E. Fiscus, H.-C. zur Loye, M.D. Amiridis, Appl. Catal. A 192 (2000) 227.
[11] S. Iijima, Nature 354 (1991) 56.
[12] K.P. de Jong, J.W. Geus, Catal. Rev.-Sci. Eng. 42 (2000) 481.
[13] S. Takenaka, H. Ogihara, K. Otsuka, J. Catal. 208 (2002) 54.
[14] W.E. Alvarez, B. Kitiyanan, A. Borgna, D.E. Resasco, Carbon 39 (2001) 547.
[15] Y. Li, J. Chen, L. Chang, Y. Qin, J. Catal. 178 (1998) 76.
[16] L.B. Avdeeva, O.V. Goncharova, D.I. Kochubey, V.I. Zaikovskii, L.M. Plyasova, B.N. Novgorodov, Sh.K. Shaikhutdinov, Appl. Catal. A 141 (1996) 117.
[17] M.A. Ermakova, D.Yu. Ermakov, G.G. Kuvshinov, L.M. Plyasova, J. Catal. 187 (1999) 77.
[18] T.B. Massalski, in: Binary Alloy Phase Diagrams, Vol. 3, 2nd ed., The Materials Information Society, OH, 1989.
[19] R.T. Yang, J.P. Chen, J. Catal. 115 (1989) 52.
[20] E. Boellaard, P.K. de Bokx, A.J.H.M. Kock, J.W. Geus, J. Catal. 96 (1985) 481.